Supporting Information

Hu et al. 10.1073/pnas.1418000111

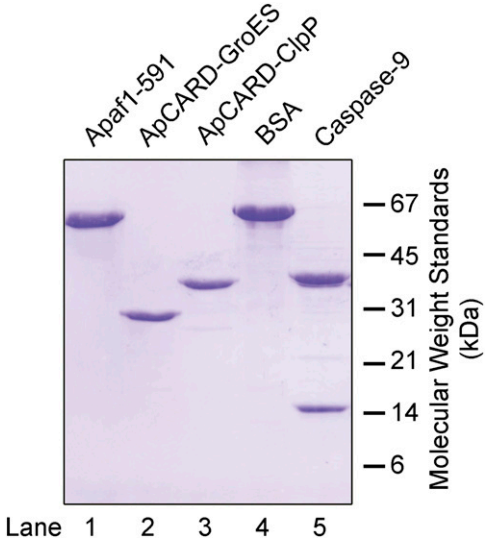

Fig. S1. Highly purified, recombinant proteins were used for mechanistic investigation of caspase-9 activation. Shown here is a representative SDS/PAGE gel visualized by Coomassie blue staining. Apaf1-591 contains residues 1–591 of Apaf-1; this protein is sufficient for formation of the apoptosome and subsequent caspase-9 activation (1). ApCARD–GroES is a fusion protein between ApCARD (residues 1–105) and GroES from *Escherichia coli* (residues 1–97). ApCARD–ClpP is a fusion protein between ApCARD (residues 1–105) and ClpP from *E. coli* (residues 1–194). BSA was purchased from Sigma and serves as a negative control. Caspase-9 shown here contains two subunits: p35 (residues 1–315) and p12 (residues 316–416).

1. Riedl SJ, Li W, Chao Y, Schwarzenbacher R, Shi Y (2005) Structure of the apoptotic protease-activating factor 1 bound to ADP. *Nature* 434(7035):926–933.

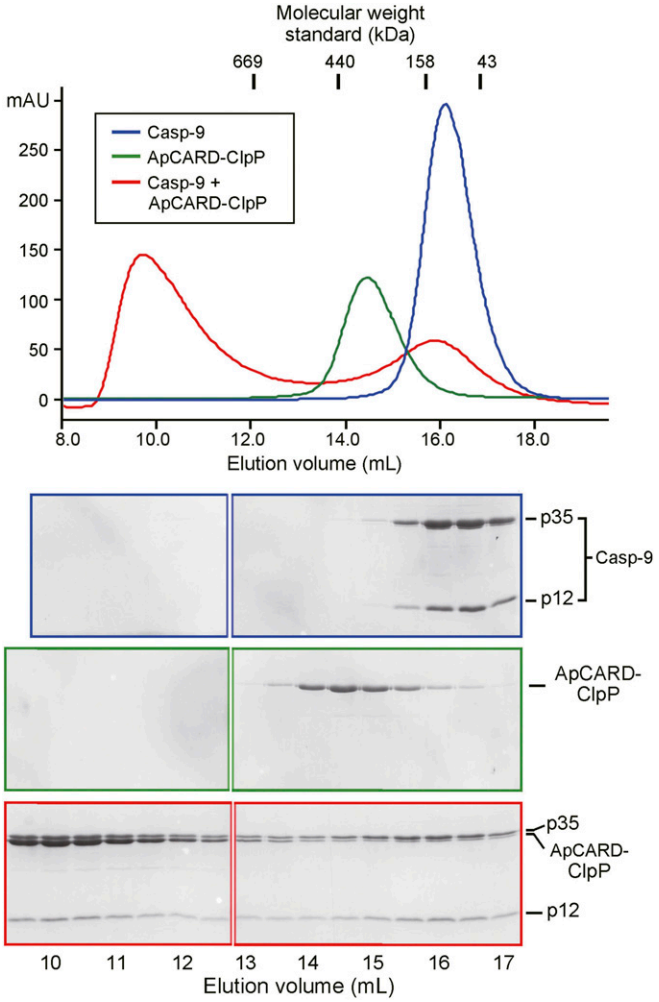

Fig. S2. Caspase-9 and the ApCARD–ClpP heptamer form a multimeric complex on gel filtration. (*Upper*) Three gel filtration chromatograms are overlaid. Blue line, caspase-9 alone; green line, ApCARD–ClpP heptamer alone; red line, caspase-9 plus ApCARD–ClpP heptamer. Incubation of caspase-9 with the heptameric ApCARD–ClpP complex resulted in the formation of a multimeric complex. Peak fractions from gel filtration were visualized by SDS/PAGE and Coomassie blue staining.

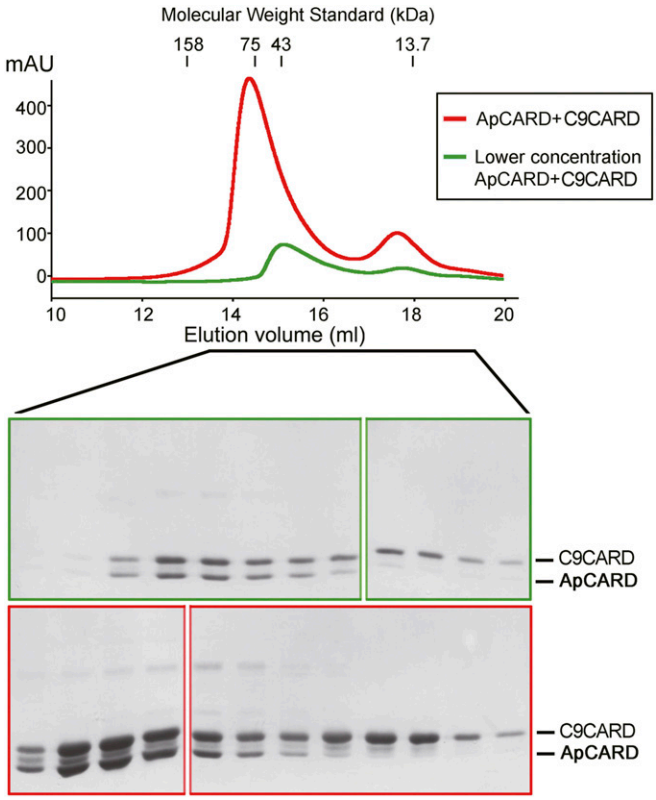

Fig. S3. The apparent molecular mass of the ApCARD–C9CARD complex changes in a concentration-dependent manner. Shown here are gel filtration chromatograms (*Upper*) and peak fractions visualized on SDS/PAGE by Coomassie blue staining (*Lower*). At the higher concentration (red line), ApCARD and C9CARD formed a complex with an apparent molecular mass of more than 75 kDa. At the lower concentration (green line), the molecular mass of the ApCARD–C9CARD complex was reduced to ~50 kDa.

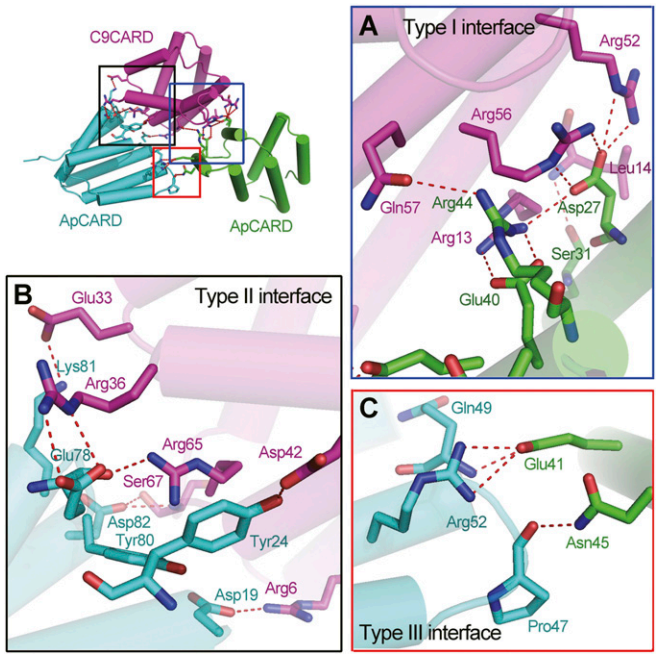

Fig. S4. Specific interactions at the three types of interfaces in the ApCARD–C9CARD complex. (*A*) Close-up view of the type I interface. H-bonds are represented by red dashed lines. The interactions observed here are nearly identical to those reported in the structure of the 1:1 complex between ApCARD and C9CARD (1). (*B*) Close-up view of the type II interface. Arg36 and Arg65 appear to anchor this interface by each making multiple interactions. The type I and type II interfaces each has a high density of H-bonds. (*C*) Close-up view of the type III interface.

1. Qin H, et al. (1999) Structural basis of procaspase-9 recruitment by the apoptotic protease-activating factor 1. *Nature* 399(6736):549–557.

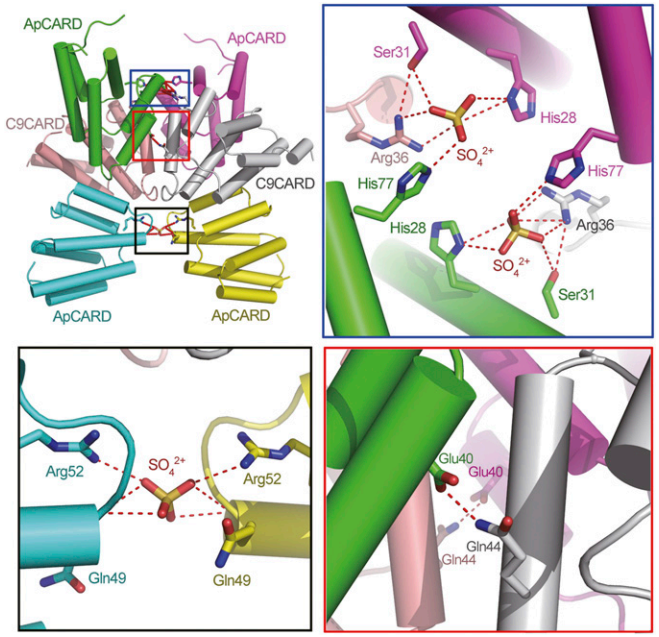

Fig. S5. The interface between two basic units of the ApCARD–C9CARD hetero-trimer is mainly mediated by sulfate ions. Three close-up views are shown. Three sulfate ions are located at the interface between two basic units of the ApCARD–C9CARD heterotrimer. A large majority of the H-bonds are mediated by these sulfate ions. Notably, two sulfate ions are located close to Ser31 of ApCARD. This observation suggests a possibility that phosphorylation of the solvent-exposed residue Ser31 may modulate CARD assembly.

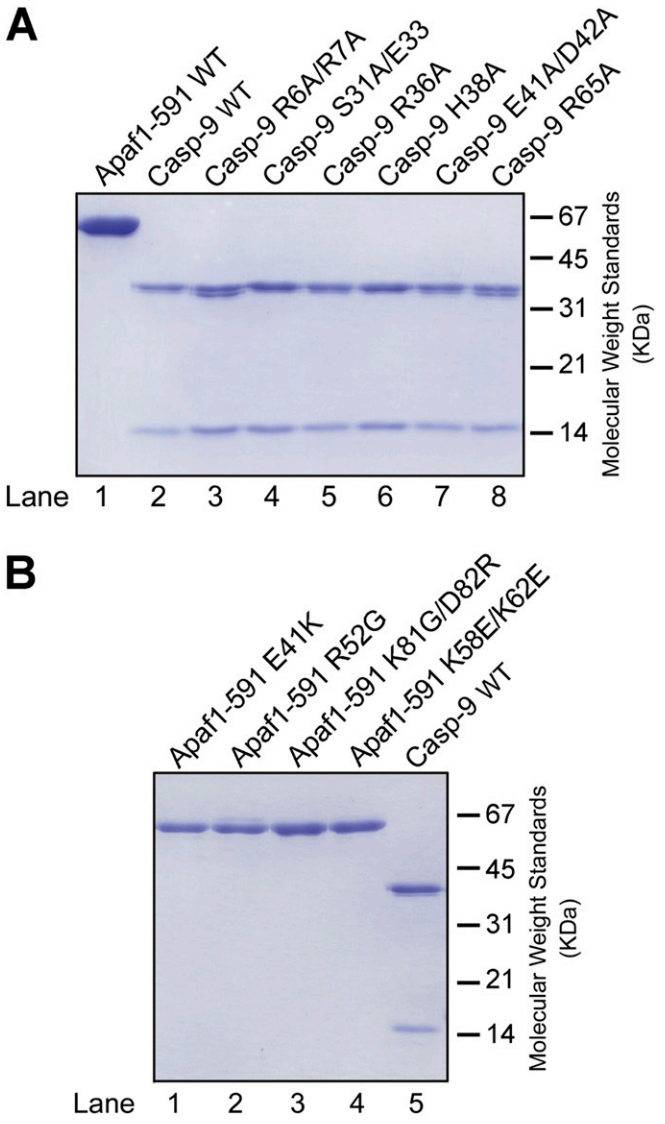

Fig. S6. Variants of caspase-9 and Apaf-1 were purified to homogeneity for biochemical characterization. (*A*) Six variants of caspase-9 were visualized on an SDS/PAGE gel by Coomassie blue staining. Each variant carries one or two missense mutations that target the type II interface. (*B*) Four variants of Apaf1-591 were visualized on an SDS/PAGE gel by Coomassie blue staining. Each variant carries one or two missense mutations that target the type II or type III interface.

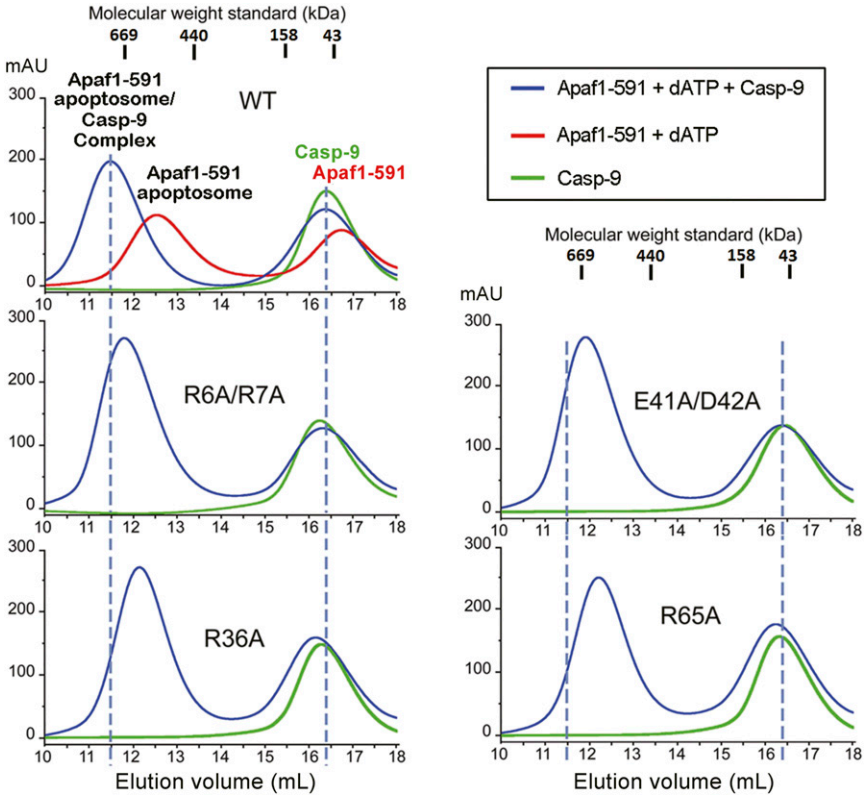

Fig. S7. Mutations in caspase-9 that target the type II interface affect formation of a multimeric complex between caspase-9 and the Apaf1-591 apoptosome. Shown here are gel filtration chromatograms for four caspase-9 variants, each with a varying degree of compromised ability to be activated by the Apaf1-591 apoptosome. The apparent molecular mass for each of the complexes between Apaf1-591 and the caspase-9 variants is smaller than that between Apaf1-591 and WT caspase-9.

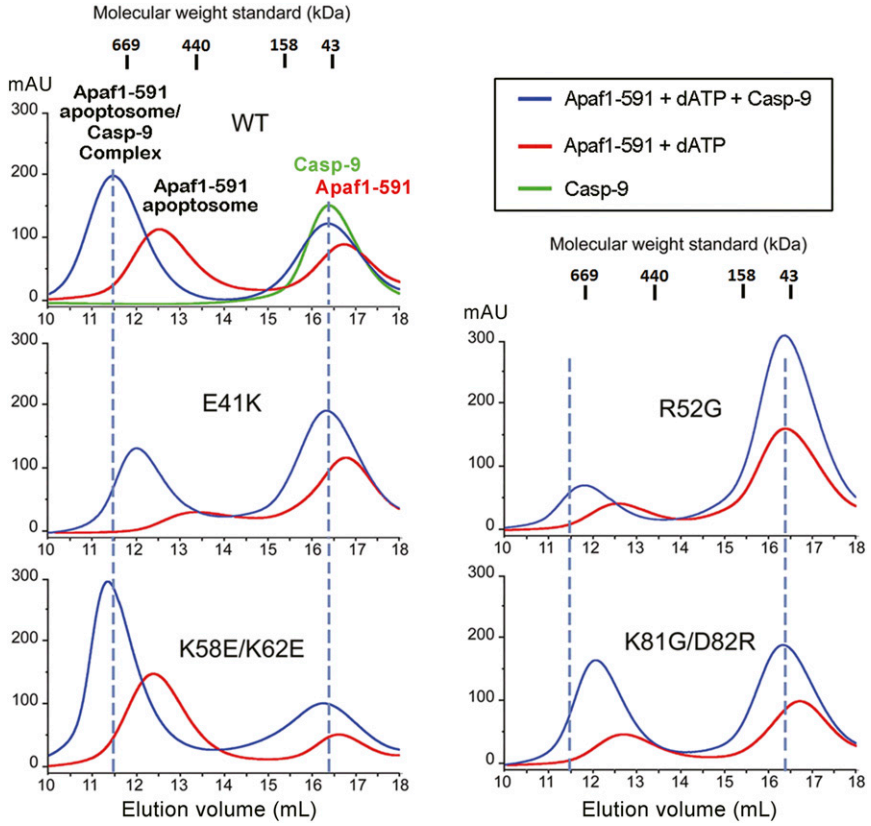

Fig. S8. Mutations in Apaf1-591 that target the type II or type III interface affect formation of a multimeric complex between caspase-9 and the Apaf1-591 apoptosome. Shown here are gel filtration chromatograms for four Apaf1-591 variants, each with a varying degree of compromised ability to activate caspase-9. For three variants, the apparent molecular mass for each of the complexes between the Apaf1-591 variant and caspase-9 is smaller than that between WT Apaf1-591 and caspase-9. Notably, for the Apaf1-591 K58E/K62E variant, the apparent molecular mass is nearly identical to that between WT Apaf1-591 and caspase-9. However, despite formation of the multimeric complex between caspase-9 and the Apaf1-591 apoptosome, Apaf1-591 K58E/K62E exhibits a severely compromised ability to activate caspase-9.

Table S1. Data collection and refinement statistics

Data	ApC9
Integration package	HKL2000
Space group	$P2_1$
Unit cell, Å	64.53, 92.52, 68.03
Unit cell, °	90, 109.12, 90
Wavelength, Å	1.5418
Resolution, Å	30∼2.10 (2.18∼2.10)
R_{merge}, %	4.9 (13.6)
I/σ	22.2 (11.0)
Completeness, %	99.7 (98.7)
No. of measured reflections	158,431
No. of unique reflections	43,908
Redundancy	3.6 (3.5)
R_{work}/R_{free}, %	21.04/22.26
No. atoms	
Protein	4,584
Main chain	2,264
Side chain	2,320
Water	355
Others	37
Average B value, Å^2	
Protein	28.60
Main chain	25.25
Side chain	31.86
Water	35.90
Others	46.43
rmsds	
Bonds, Å	0.013
Angle, °	1.123
Ramachandran plot statistics, %	
Most favorable	95.6
Additionally allowed	4.4
Generously allowed	0.0
Disallowed	0.0

Values in parentheses are for the highest resolution shell. $R_{merge}=\Sigma_h\Sigma_i|I_{h,i}-I_h|/\Sigma_h\Sigma_i I_{h,i}$, where I_h is the mean intensity of the i observations of symmetry related reflections of h. $R = \Sigma||F_{obs}|-|F_{calc}||/\Sigma|F_{obs}|$, where F_{calc} is the calculated protein structure factor from the atomic model (R_{free} was calculated with 5% of the reflections selected).